Acta Math. Univ. Comenianae
Vol. LXVII, 1(1998), pp. 137–157

MAXIMUM PRINCIPLE AND LOCAL MASS BALANCE FOR NUMERICAL SOLUTIONS OF TRANSPORT EQUATION COUPLED WITH VARIABLE DENSITY FLOW

P. FROLKOVIČ

Abstract. A parabolic convection-diffusion equation of the transport in porous media strongly coupled with a flow equation through a variable fluid density is studied from the point of view of the qualitative properties of numerical solution. A numerical discretization is based on "node-centered" finite volume methods with a clear form for a local mass balance property. Numerical solutions of the discrete conservation laws fulfill a discrete maximum (and minimum) principle. The presented results are an extension of ones in [**12**], [**7**] and [**1**] for the case of transport equation coupled with variable density flow including the source/sink terms, inflow/outflow boundary conditions and anisotropic diffusion and for the case of upwind algorithms applied to a general class of finite volume meshes.

1. Introduction and Mathematical Model

A motivation of the following mathematical problem arises from the area of modelling the groundwater flows near salt domes where the fluid is supposed to be a mixture of two components – **pure water** and **brine** (concentrated salt water). Although we do not plan to describe in details the derivation of the model, see [**10**], [**13**] or [**11**], we mention here some of its important characteristics.

Accepting first that the displacement of single-phase components is **miscible** (i.e. each liquid can occupy the same portion of the space at the same time) and taking into account the (large) difference between the density of pure water and brine (more then 20%), a variability of the fluid mixture density ρ can be then expressed by a functional dependence on the mass fraction of one of the components.

Introducing a velocity $\mathbf{q}$ of the fluid as a **mass averaged** velocity of each component and applying the standard concept of porous media, we arise from a mass conservation law for the fluid mixture to the equation for **variable density flow**

$$\phi\partial_t\rho + \nabla\cdot(\rho\mathbf{q}) + \rho Q^- = \rho^+ Q^+ \tag{1}$$

Received July 1, 1997.
1980 *Mathematics Subject Classification* (1991 *Revision*). Primary 65M60; Secondary 80A20.
Key words and phrases. Parabolic convection-diffusion equations, finite volume methods, upwind, artificial diffusion, discrete maximum principle, conservation laws.

where the velocity $\mathbf{q}$ is **explicitly** given by Darcy's law

$$\mathbf{q} = -\frac{K}{\mu}\left(\nabla p - \rho \mathbf{g}\right) \tag{2}$$

and where the unknown function $p = p(x,t)$ is the **pressure** of the fluid.

Finally, denoting the unknown function $c = c(x,t)$ to be the mass fraction (**concentration**) of the brine component, we end with a parabolic convection-diffusion equation of the transport in porous media

$$\phi \partial_t(\rho c) + \nabla \cdot (\rho c \mathbf{q} - \rho D \cdot \nabla c) + \rho c Q^- = \rho^+ c^+ Q^+ \tag{3}$$

where the strong coupling of all equations is realized especially through the dependence of the fluid density $\rho = \rho(c)$ on the brine concentration c where $\rho \geq \rho_w > 0$ with ρ_w being the density of pure water.

As we neglect a compressibility of the fluid by no dependence of ρ on p, we can characterize the equations (1) and (3) as a parabolic-elliptic system for the unknown functions c and p.

Other data of the model include the porosity $\phi = \phi(x) \in (0,1\rangle$, the sink term $Q^- = Q^-(x,t) \geq 0$ and the source term $Q^+ = Q^+(x,t) \geq 0$ with $c^+ = c^+(x,t)$ being a given concentration of the externally supplied brine by the fluid of the density $\rho^+ (:= \rho(c^+))$. Further $K = K(x)$ is the permeability tensor, $\mu = \mu(c)$ is the viscosity of the fluid and $\mathbf{g}$ is the constant gravity vector.

Finally, the anisotropic tensor D includes the effects of molecular diffusion and tortuosity and in general the velocity-dependant dispersion effects. Further we simplify $D = D(x)$ to be a "diffusion" tensor that is always for fixed values represented by a symmetric positive definite matrix.

The equations are considered for $x \in \Omega \subset R^2$ where Ω is a polygonal domain and $t \in (0,T)$, $T > 0$ and they are accompanied with the initial conditions for c

$$c(x,0) = c^0(x)\,,\ x \in \Omega \tag{4}$$

and with the Dirichlet boundary conditions for c on one part of the boundary $\Gamma^D \subset \partial\Omega$

$$c(x,t) = c^D(x,t), \quad x \in \Gamma^D, \quad t \in (0,T) \tag{5}$$

and with so called "inflow/outflow" boundary conditions on the other part $\Gamma^I \cup \Gamma^O$. For the "inflow" boundary $\Gamma^I := \{x \in \partial\Omega \backslash \Gamma^D, \mathbf{n} \cdot \mathbf{q} \leq 0\}$ with $\mathbf{n} = \mathbf{n}(x)\,,\ x \in \partial\Omega$ being an outer unit normal, we set

$$\rho \mathbf{n} \cdot (\mathbf{q} c - D \cdot \nabla c) = \rho^I \mathbf{n} \cdot \mathbf{q} c^I\,,\ \ x \in \Gamma^I \tag{6}$$

and for the "outflow" boundary $\Gamma^O := \{x \in \partial\Omega \backslash \Gamma^D , \mathbf{n} \cdot \mathbf{q} > 0\}$ we set

$$\rho \mathbf{n} \cdot (\mathbf{q}c - D \cdot \nabla c) = \rho \mathbf{n} \cdot \mathbf{q}c \,, \quad x \in \Gamma^O \,. \tag{7}$$

Analogously to the source/sink terms formulation we suppose that the inflow boundary acts as a source supplying a given concentration c^I and the outflow boundary as a sink carrying the actual concentration c. Isolated boundaries ("zero flux") are for a simplicity included in Γ^I.

The boundary conditions (6) are very often replaced by (not equivalent) Dirichlet boundary conditions where c is directly set to c^I at Γ^I, i.e.

$$c(x,t) = c^I(x,t), \quad x \in \Gamma^I . \tag{8}$$

In general we can consider for p independently the Dirichlet boundary conditions at some part of $\partial\Omega$ and the flux dependent boundary conditions at another part, what we do not specify precisely here.

It is worth to note that by neglecting the variability of ρ and other data on c the flow equation (1) turns to a stationary Poisson equation for so called "piezometric head" [**4**]. Such equation needs to be solved only once and the computed velocity $\mathbf{q}$ can be then put into the transport equation (3) that itself turns to a parabolic **linear** convection-diffusion equation.

Such models are well studied in literature, see for instance [**7**] and [**1**] where also results about discrete maximum principles can be found for the case of convection dominated transport with some upwind techniques applied. Considering $\rho = \rho(c)$ the simplifications are no more possible and the model has to be studied in the form (1)–(3). Nevertheless, as it will be presented in this paper, the results can be successfully extended.

2. Finite Volume Methods

Finite element methods (FEM) have gained their good reputation due to the applicability to diverse problems where complex geometries and general data do not allow simplifications used previously for finite difference methods. Many nontrivial features like anisotropy of the data or flux dependant boundary conditions are in natural way included into a finite element formulation.

To still profit from the advantages of FEM and to enhance them by introducing a property of **local mass balance**, we concentrate here on the class of finite volume methods (FVM) that are closely related to conforming finite element methods.

Following the approach of FEM we start with an **admissible triangulation** [**1**] $\mathcal{T}$ of Ω where we restrict ourselves only to triangle elements.

We use further the following notations: $e \in \Lambda$ where e is the index of all elements $T^e \in \mathcal{T}$; $i = 1, \ldots, N$ where i is the index for all vertices $x_i \in \Omega$ of $\mathcal{T}$ and N is the number of the vertices of the triangulation; $i \in \Lambda^e$ where i is the index for all

$x_i \in T^e$; $j \in \Lambda_i$ where j is the index of all neighbour vertices x_j to x_i; $\Lambda_i^e := \Lambda^e \cap \Lambda_i$ and $e \in \Lambda_{ij}$ where e is the index of (one or two) elements containing the vertices x_i and x_j .

The number of the vertices of the triangulation excluding ones at $\partial\Omega$ we denote by I ($I < N$), where we suppose that for some J ($I \le J \le N$) we have $x_j \in \Gamma^D$, $j = J+1,\dots,N$. By $j \in \Lambda_i^b$ we mean all indices $j \in \Lambda_i$ such that $x_j \in \partial\Omega$, by $j \in \Lambda_i^I$, resp. $j \in \Lambda_i^O$ such that $j \in \Lambda_i$ and $x_j \in \Gamma^I$, resp. $x_j \in \Gamma^O$.

To discretize the time interval $(0,T)$ we introduce for a simplicity a constant time step $\tau := T/M$ and we denote $t_m := m\tau$, $m = 0,\dots,M$.

Having the discrete form of space and time domain we associate each x_i and t_m with unknown value c_i^m that should be determined as a numerical approximation of c

$$c_i^m \approx c(x_i,t_m)\,,\ i = 1,\dots,J\,,\ m = 1,\dots,M\,. \tag{9}$$

We omit often, if possible, the index m, i.e. $c_i := c_i^m$.

The Dirichlet boundary conditions (5) we apply directly by

$$c_j^m := c^D(x_j,t_m)\,,\ j = J+1,\dots,N\,,\ m = 1,\dots,M \tag{10}$$

and similarly the initial conditions by

$$c_i^0 := c^0(x_i)\,,\ i = 1,\dots,N\,. \tag{11}$$

To derive algebraic equations for the unknowns c_i^m we leave the approach of FEM and we introduce a concept of **local mass balance** property.

The equation (1) represents a differential form of mass conservation law, so for any $V \subset \Omega$ and $(t_{m-1},t_m) \subset (0,T)$ we obtain by integration of (1) and by the application of Green's formula the following integral formulation

$$\begin{aligned}\int_V (\phi\rho)(t_m)\,dx = {} & \int_V (\phi\rho)(t_{m-1})\,dx - \int_{t_{m-1}}^{t_m}\int_{\partial V} \rho\mathbf{n}\cdot\mathbf{q}\,d\gamma\,dt \\ & + \int_{t_{m-1}}^{t_m}\int_V \left(\rho^+Q^+ - \rho Q^-\right)\,dx\,dt\,.\end{aligned} \tag{12}$$

The equation (12) represents a local mass balance in the sense that the mass of fluid in the volume V of porous media at the time t_m is equal to the mass in V at t_{m-1} with the changes due to the addition/subtraction of the mass caused by a flux through the boundary ∂V and source/sink terms during the time interval (t_{m-1},t_m).

Similar interpretation has the equation

$$\begin{aligned}\int_V (\phi\rho c)(t_m)\,dx = {} & \int_V (\phi\rho c)(t_{m-1})\,dx - \int_{t_{m-1}}^{t_m}\int_{\partial V} \rho\mathbf{n}\cdot(c\mathbf{q} - D\cdot\nabla c)\,d\gamma\,dt \\ & + \int_{t_{m-1}}^{t_m}\int_V \left(\rho^+c^+Q^+ - \rho c Q^-\right)\,dx\,dt\end{aligned} \tag{13}$$

if we take into account that ρc is equal to the density of brine component.

The idea of **"node centered"** finite volume methods is to associate with each vertex x_i (and in general for each time t_m) a finite volume V_i (with "node" x_i being a "center" of V_i) for which the equations (12) and (13) have to be fulfilled in some discrete form.

Remark 2.1. It is important to note that (12) and (13) will represent for FVM a local mass balance at the "smallest scale". To have a reasonable procedure to extend it further to any union of finite volumes and time intervals, including the limit case $\Omega \times (0, T)$, we have to follow some guidelines.

First, if the grid changes in time, i.e. the vertices for c_i^{m-1} and c_i^m do not necessary correspond to each other, one should insure that no mass changes are introduced by an interpolation, resp. restriction of the numerical solution between two different grids (for a fixed grid the problem does not appear).

Although for a general situation it is difficult to formulate this property "locally", it has a clear form for the "global" level where one should preserve for both grids the value of mass in the whole domain

$$\bigcup_{i=1,\ldots,N} \int_{V_i} (\phi\rho)(t_m)\, dx.$$

Further, to extend the mass conservation in space a compatibility of the fluxes between adjacent finite volumes V_i and V_j must be fulfilled. This condition will be in our approach automatically fulfilled.

To construct the dual mesh of finite volumes V_i, $i = 1, \ldots, N$ we define further a reasonably general form of V_i with all well-known choices included.

The dual mesh will be uniquely determined by a choice of point $x^e \in T^e$ for each element of the triangulation. Denoting then x_{ij} the midpoint of the edge connecting x_i and x_j, we can define Γ_{ij}^e to be the line segment between the points x^e and x_{ij}, $i, j \in \Lambda^e$ and we define

$$\Gamma_i := \bigcup_{j\in\Lambda_i} \bigcup_{e\in\Lambda_{ij}} \Gamma_{ij}^e\,,\ i = 1, \ldots, N.$$

Moreover, for $i = I + 1, \ldots, N$ we connect the points x_i and x_{ij}, $j \in \Lambda_i^b$ by the line segment $\Gamma_{ij}^b \in \partial\Omega$ and we define

$$\Gamma_i^b := \bigcup_{j\in\Lambda_i^b} \Gamma_{ij}^b\,,\ \ i = I + 1, \ldots, N.$$

The finite polygon surrounded by Γ_i, resp. by $\Gamma_i \cup \Gamma_i^b$, we denote as the **finite volume** V_i.

In general $x^e \notin \partial T^e$ except the case when x^e coincides with one of the points x_{ij} when we have then the limit case $\Gamma_{ij}^e = \{x_{ij}\}$.

It is clear that we have

$$V_i \neq \emptyset\,,\ i = 1, \ldots, N \ \ \& \ \ \bar{\Omega} = \bigcup_{i=1,\ldots,N} \bar{V}_i .$$

We present details for two types of mostly used dual meshes of finite volumes and a motivation for a general case, see the Figure 1 for a comparison.

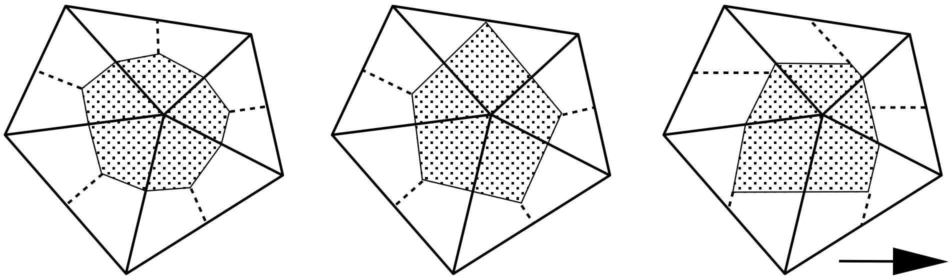

Figure 1. Donald, Voronoi and Aligned finite volumes.

The choice of so called **Donald diagrams** [**1**] by considering $x^e = x_B^e$ where x_B^e is the **barycenter** of T^e

$$x_B^e := \frac{1}{3} \sum_{i \in \Lambda^e} x_i$$

has several geometric advantages. It is applicable with no restrictions on the triangulation and it divides each T^e into 3 subregions with the same area.

By setting $x^e = x_C^e$ with x_C^e being the **circumcenter** of T^e

$$x_C^e : \ |x_C^e - x_i| = |x_C^e - x_j|\,, \quad \forall i, j \in \Lambda^e ,$$

i.e. x_C^e is the point equidistant with respect to all vertices of T^e, we get so called **Voronoi diagrams** [**1**] that, as wee see later, have good approximation properties. The construction however, to have $x_C^e \in T^e$, is restricted to so called **weakly acute** triangulation where each triangle has no angle greater then $\pi/2$. The point x_C^e can coincide with one of the points x_{ij}, otherwise the segment Γ_{ij}^e is perpendicular to the edge connecting points x_i and x_j.

We consider also a general and variable situation for x^e to allow for instance so called **aligned** finite volumes that are constructed with the purpose to align the line segments Γ_{ij}^e to some given direction. The main application is the alignment with respect to the convective velocity field, see [**2**] and [**8**].

3. Finite Volume Discretizations

To construct a discrete form of the analytical mass balance equations (12) and (13) over a finite volume V_i and a time interval (t_{m-1}, t_m) we have to "extend" the nodal values c_i^m by assuming some interpolation profile over the domain of definition in each integral. Here we can profit from one of the main advantages of "node-centered" FVM by applying an interpolation used in FEM.

To be able to evaluate in discrete form ∇c we use (continuous) piecewise "linear" interpolation $\tilde{c}$ of the form:

$$\tilde{c} = \tilde{c}(x) := \tilde{c}^m(x) := \sum_{i=1}^{N} c_i^m N_i(x)\,,\ x \in \Omega \tag{14}$$

where N_i are the standard "linear" basis functions with $N_i(x_j) = \delta_{ij}$. We denote $\nabla N_i^e := \nabla N_i|_{T^e}$ and inside of each element we get a **constant** vector for the gradient of $\tilde{c}$

$$\nabla \tilde{c}(x) \equiv \sum_{i \in \Lambda^e} c_i \nabla N_i^e\,,\ x \in T^e\,.$$

Next, by $|\Gamma_{ij}^e|$ we denote the length of Γ_{ij}^e inclusive the case $|\Gamma_{ij}^e| = 0$, by $\mathbf{n}_{ij}^e$ (if $|\Gamma_{ij}^e| \neq 0$) we denote the unit outer normal w.r.t. $\Gamma_{ij}^e \subset \partial V_i$ having naturally $\mathbf{n}_{ij}^e \equiv -\mathbf{n}_{ji}^e$. Similarly by $\mathbf{n}_{ij}^b$ we denote the unit outer normal w.r.t. $\Gamma_{ij}^b \subset \partial\Omega$. We strictly consider further that $|\Gamma_{ij}^e| \neq 0$ where for the limit case $\Gamma_{ij}^e = \{x_{ij}\}$ all next considerations can be simply omitted.

We fix the values of D and ρ per each element, for instance by

$$D^e := D(x_B^e)\,,\ \rho^e = \rho(x_B^e)\,,\ e \in \Lambda$$

where for nonlinear data we mean $\rho(x_B^e) = \rho(c(x_B^e))$.

Now we are ready to introduce an important relation between FEM and node-centered FVM that states an equivalence of both discretizations for the case of homogeneous diffusion equation. More precisely, denoting $|T^e|$ the area of the triangle T^e we have for $i = 1, \ldots, N$ and $j \in \Lambda_i$

$$|T^e|(\nabla N_i^e)^T \cdot D^e \cdot \nabla N_j^e = -\sum_{l \in \Lambda_i^e} (|\Gamma_{il}^e|\mathbf{n}_{il}^e) \cdot D^e \cdot \nabla N_j^e \tag{15}$$

where l.h.s. of (15) is the basic scalar product of FEM discretization.

The above statement can be found in [**7**], [**6**] and [**1**] where only scalar case $D^e = d^e I$ is studied, but the proof can be simply extended for the case of a symmetric positive definite matrix D^e.

Next we introduce the important notation

$$\lambda_{ij}^e := \begin{cases} h_{ij}|\Gamma_{ij}^e|^{-1} \sum_{l \in \Lambda_i^e} (|\Gamma_{il}^e|\mathbf{n}_{il}^e) \cdot D^e \cdot \nabla N_j^e & |\Gamma_{ij}^e| \neq 0 \\ 0 & |\Gamma_{ij}^e| = 0 \end{cases} \tag{16}$$

where $h_{ij} = |x_i - x_j|$ denotes the length of the edge between x_i and x_j. Due to (15) and the symmetry of D^e we have $\lambda^e_{ij} = \lambda^e_{ji}$. Now we are ready to introduce two equivalent approximations of the diffusive flux

$$
\begin{aligned}
(17)\qquad & -\int_{\partial V_i \cap T^e} \mathbf{n} \cdot D \cdot \nabla c \, d\gamma \approx -\int_{\partial V_i \cap T^e} \mathbf{n} \cdot D^e \cdot \nabla \tilde{c} \, d\gamma \\
& \qquad = -\sum_{l \in \Lambda^e_i} (|\Gamma^e_{il}| \mathbf{n}^e_{il}) \cdot D^e \cdot \sum_{k \in \Lambda^e} c_k \nabla N^e_k = \sum_{l \in \Lambda^e_i} |\Gamma^e_{il}| \, \lambda^e_{il} \frac{c_i - c_l}{h_{il}}
\end{aligned}
$$

where we have used also the simple relation

$$
(18)\qquad \nabla N^e_i = -\sum_{l \in \Lambda^e_i} \nabla N^e_l \, .
$$

The first formulation of the approximation in (17) is more common and straightforward approach in FVM, but the second one in (17) will help us later to formulate upwind algorithms for a general class of FVM and for a general form of a diffusion tensor D.

Using so successfully the assumption of linear interpolation (14) to discretize ∇c one could suggest to use it to approximate all integrals, although **no** further derivatives of c appear in (12) and (13). Similarly a linear interpolation in time could be considered.

We have to emphasize that the mentioned approach requires strong restrictions on time and space discretization steps to exclude numerical instabilities [**12**], [**7**]. We rather prefer an approach of [**12**] where an aim is to have "physically reasonable" numerical solutions even for the case of coarser grids and larger time steps.

The main principle can be formulated to consider always an appropriate interpolation for the extensions of nodal values in the domain of definition of each integral in (12) and (13) that will result in a piecewise *constant* profile of the integral terms. Note that by fixing D per each element T^e and by using the linear interpolation for nodal values of c , we got **constant** approximations of all diffusive fluxes in T^e.

To evaluate integrals over $V_i \times (t_{m-1}, t_m)$ we accept that c preserves there the **constant** value c^m_i, so we get for instance

$$
\int_{t_{m-1}}^{t_m} \int_{V_i} \rho c Q^- \, dx \, dt \approx \tau |V_i| (\rho Q^-)^m_i c^m_i
$$

where $(\rho Q^-)^m_i$ stands for some approximation of the integral

$$
(\rho Q^-)^m_i \approx (\tau |V_i|)^{-1} \int_{t_{m-1}}^{t_m} \int_{V_i} \rho Q^- \, dx \, dt
$$

with an "arbitrary" order of precision with the simplest choice being

$$(\rho Q^-)_i^m = \rho_i Q_i^- := \rho(c_i^m)\, Q^-(x_i, t_m).$$

Similarly we could proceed with other terms that are integrated over V_i and (t_{m-1}, t_m).

Finally, we have to suggest an approximation of the convective flux over Γ_{ij}^e. Taking into account that the convection there expresses the exchange of mass between finite volumes V_i and V_j, we accept here a natural approach that the concentration for the convective flux at Γ_{ij}^e will be determined from some interpolation profile of c on the edge connecting x_i and x_j, i.e. depending only on the values c_i and c_j.

The approach with **no upwind** applied can be considered then as a preserving the **linear** interpolation (14) when we obtain

$$\int_{\Gamma_{ij}^e} \mathbf{n}\cdot\mathbf{q}\, c\, ds \approx \int_{\Gamma_{ij}^e} \mathbf{n}\cdot\mathbf{q}_{ij}^e\, \tilde{c}\, ds = |\Gamma_{ij}^e|\mathbf{n}_{ij}^e \cdot \mathbf{q}_{ij}^e\, \frac{c_i + c_j}{2} \tag{19}$$

and where $\mathbf{q}_{ij}^e$ represents

$$\mathbf{q}_{ij}^e \approx |\Gamma_{ij}^e|^{-1} \int_{\Gamma_{ij}^e} \mathbf{q}\, d\gamma\,. \tag{20}$$

For the case of so called "consistent velocity approximation" of (2) is $\mathbf{q}$ approximated by constant vectors per each element [**9**].

Full upwind is mostly understood as the substitution of (19) by evaluating the concentration at an **upstream** point x_i, resp. x_j, depending on the direction of the velocity $\mathbf{q}_{ij}^e$ with respect to Γ_{ij}^e, i.e.

$$\int_{\Gamma_{ij}^e} \mathbf{n}\cdot\mathbf{q}\, c\, ds \approx |\Gamma_{ij}^e|\mathbf{n}_{ij}^e \cdot \mathbf{q}_{ij}^e \left((1/2 + \gamma_{ij}^e)c_i + (1/2 - \gamma_{ij}^e)c_j\right) \tag{21}$$

where

$$\gamma_{ij}^e = \begin{cases} 1/2 & \mathbf{n}_{ij}^e \cdot \mathbf{q}_{ij}^e \geq 0, \\ -1/2 & \mathbf{n}_{ij}^e \cdot \mathbf{q}_{ij}^e < 0. \end{cases} \tag{22}$$

Such explanation is equivalent to the consideration of the **constant** profile of c between x_i and x_j with a choice of upstream value c_i, resp. c_j.

More appropriate upwind techniques, having still the form (21), will be introduced in the Section 5, where an interpolation profile of c will be suggested that gives a **constant** value of the **total** flux made of convection and diffusion on the edge between x_i and x_j.

Accepting all above assumptions we get the following discrete equations for $i = 1, \dots, N$ that represent the discrete form of mass conservation law (13) of the transport equation (3)

$$
\begin{aligned}
|V_i|\phi_i(\rho_i c_i - \rho_i^{m-1} c_i^{m-1}) + \tau \sum_{j \in \Lambda_i} \sum_{e \in \Lambda_{ij}} |\Gamma_{ij}^e| \rho^e J_{ij}^e \\
+ \tau \sum_{j \in \Lambda_i^b} |\Gamma_{ij}^b| \rho_{ij} J_{ij}^b + \tau |V_i| \, \rho_i Q_i^- c_i = \tau |V_i| \, \rho_i^+ Q_i^+ c_i^+
\end{aligned} \tag{23}
$$

Here we have used the notation for the flux J_{ij}^e

$$
J_{ij}^e := \mathbf{n}_{ij}^e \cdot \left(\mathbf{q}_{ij}^e \left((1/2 + \gamma_{ij}^e) c_i + (1/2 - \gamma_{ij}^e) c_j \right) - D^e \cdot \sum_{l \in \Lambda^e} c_l \nabla N_l^e \right) \tag{24}
$$

and the notation for the boundary fluxes J_{ij}^b

$$
J_{ij}^b :\approx \mathbf{n}_{ij}^b \cdot \left(\mathbf{q}_{ij}^b c - D \cdot \nabla c \right). \tag{25}
$$

The fluxes (25) are actually used only for the case of inflow/outflow boundary conditions (6) and (7) when with $\rho_{ij} := \rho(c(x_{ij}))$ they are substituted by

$$
\rho_{ij} J_{ij}^b = \begin{cases} \rho_{ij}^I \mathbf{n}_{ij}^b \cdot \mathbf{q}_{ij}^b c_i^I & \mathbf{n}_{ij}^b \cdot \mathbf{q}_{ij}^b \le 0, \\ \rho_{ij} \mathbf{n}_{ij}^b \cdot \mathbf{q}_{ij}^b c_i & \mathbf{n}_{ij}^b \cdot \mathbf{q}_{ij}^b > 0. \end{cases} \tag{26}
$$

The discrete form of the mass conservation law (12) for the flow equation (1) must be discretizied in the analogous form

$$
\begin{aligned}
|V_i|\phi_i(\rho_i - \rho_i^{m-1}) + \tau \sum_{j \in \Lambda_i} \sum_{e \in \Lambda_{ij}} |\Gamma_{ij}^e| \rho^e \mathbf{n}_{ij}^e \cdot \mathbf{q}_{ij}^e \\
+ \tau \sum_{j \in \Lambda_i^b} |\Gamma_{ij}^b| \rho_{ij} \mathbf{n}_{ij}^b \cdot \mathbf{q}_{ij}^b + \tau |V_i| \, \rho_i Q_i^- = \tau |V_i| \, \rho_i^+ Q_i^+
\end{aligned} \tag{27}
$$

with some discrete form of Darcy's law (2) for $\mathbf{q}_{ij}^e$ that we do not specify here (see [**9**] and [**5**] for the consistent velocity approximation).

For the case of Dirichlet boundary conditions for c the equations (23) need not to be included into the computations and the values c_i^m are for $i = J+1, \dots, N$ determined directly from (10). Nevertheless these equations can be used afterwards ("postprocessing") to compute the unknown fluxes J_i^b over Γ^D where by J_i^b we understand a sum of the fluxes J_{ij}^b and J_{ik}^b, $j, k \in \Lambda_i^b$.

Further, as we see in the next sections, it is important that the equations (27) are fulfilled also for $i = I+1, \dots, J$ independently of the type of boundary conditions for p.

4. Discrete Maximum Principle

Before starting any considerations about a discrete maximum principle we have to emphasize that also geometric properties of the grid influence considerably a qualitative behaviour of numerical solution.

As we see later an important property is the sign of λ_{ij}^e defined by (16) that represents for us "discrete characteristics" of a diffusion associated with the nodes x_i and x_j in the element T^e. For the case of diagonal diffusion matrix $D = dI$ it can be shown [**7**], [**1**] that for weakly acute triangulation (no triangle with an angle greater then $\pi/2$) we have $\lambda_{ij}^e \geq 0$, $e \in \Lambda$, $i, j \in \Lambda^e$, $i \neq j$.

We assume further that the triangulation $\mathcal{T}$ preserves this property also for a fixed (anisotropic symmetric positive definite) matrix D^e per each element, i.e.

$$(\nabla N_i^e)^T \cdot D^e \cdot \nabla N_j^e \geq 0\,,\ \forall e \in \Lambda\,,\ i, j \in \Lambda^e\,,\ i \neq j\,. \tag{28}$$

Using then (15) we have $\lambda_{ij}^e \geq 0$ and moreover $\lambda_{ij}^e = \lambda_{ji}^e$ due to the symmetry of D^e.

We emphasize that (28) is determined only by geometric properties of the grid and by a "character" of the anisotropy for D^e and for the case of isotropic diffusion it is purely geometric property of the triangulation.

Now we are ready to formulate an important property of the numerical solution.

Theorem 4.1. *Let c_i $(:= c_i^m)$, $i = 1, \ldots, J$ fulfill the equations* (23) *and let the equations* (27) *hold. If the triangulation $\mathcal{T}$ preserves the property* (28) *then the* **discrete maximum** *(and* **minimum***)* **principle** *is fulfilled, i.e.*

$$c_i \leq \max\left\{ \max_{j=J+1,\ldots,N}\{c_j\}\,,\ \max_{j'}\{c_j^+\}\,,\ \max_{j'}\{c_j^I\}\,,\ \max_{j=1,\ldots,J}\{c_j^{m-1}\} \right\}\,; \tag{29}$$

$$c_i \geq \min\left\{ \min_{j=J+1,\ldots,N}\{c_j\}\,,\ \min_{j'}\{c_j^+\}\,,\ \min_{j'}\{c_j^I\}\,,\ \min_{j=1,\ldots,J}\{c_j^{m-1}\} \right\} \tag{30}$$

where by j', $1 \leq j' \leq J$ we denote all indices where $Q_{j'}^+ > 0$, resp. $x_{j'} \in \Gamma^I$.

Proof. We prove only (30) as (29) can be proved analogously.

Let $c_i := \min_{j=1,\ldots,J}\{c_j\}$, i.e. $1 \leq i \leq J$. We suppose next that

$$c_i < \min_{j=1,\ldots,N}\{c_j\} \tag{31}$$

because otherwise (30) follows trivially.

Using (17) we rewrite (23) to the equivalent form

$$
\begin{aligned}
&c_i\Big(|V_i|\phi_i\rho_i + \tau|V_i|\rho_i Q_i^- + \tau\sum_{j\in\Lambda_i}\sum_{e\in\Lambda_{ij}}|\Gamma_{ij}^e|\rho^e\Big((\gamma_{ij}^e+1/2)\mathbf{n}_{ij}^e\cdot\mathbf{q}_{ij}^e + \lambda_{ij}^e h_{ij}^{-1}\Big)\\
&\quad + \tau\sum_{j\in\Lambda_i^O}|\Gamma_{ij}^b|\rho_{ij}\mathbf{n}_{ij}^b\cdot\mathbf{q}_{ij}^b\Big)\\
&= c_i^{m-1}|V_i|\phi_i\rho_i^{m-1} + c_i^+\tau|V_i|\rho_i^+Q_i^+ + c_i^I\tau\sum_{j\in\Lambda_i^I}|\Gamma_{ij}^b|\rho_{ij}^I\mathbf{n}_{ij}^b\cdot\mathbf{q}_{ij}^b\\
&\quad + \tau\sum_{j\in\Lambda_i}c_j\left(\sum_{e\in\Lambda_{ij}}|\Gamma_{ij}^e|\rho^e\Big((\gamma_{ij}^e-1/2)\mathbf{n}_{ij}^e\cdot\mathbf{q}_{ij}^e+\lambda_{ij}^e h_{ij}^{-1}\Big)\right).
\end{aligned}
\tag{32}
$$

Summarizing all properties of the data and the grid we can claim that all coefficients of c_i, c_j, c_i^{m-1}, c_i^+ and c_i^I are nonnegative.

Using now (31) we can substitute each c_j in (32) by c_i to obtain after some simplifications the estimate

$$
\begin{aligned}
&c_i\Big(|V_i|\phi_i\rho_i + \tau|V_i|\rho_i Q_i^- + \tau\sum_{j\in\Lambda_i}\sum_{e\in\Lambda_{ij}}|\Gamma_{ij}^e|\rho^e\mathbf{n}_{ij}^e\cdot\mathbf{q}_{ij}^e + \tau\sum_{j\in\Lambda_i^O}|\Gamma_{ij}^b|\rho_{ij}\mathbf{n}_{ij}^b\cdot\mathbf{q}_{ij}^b\Big)\\
&\geq c_i^{m-1}|V_i|\phi_i\rho_i^{m-1} + c_i^+\tau|V_i|\rho_i^+Q_i^+ + c_i^I\tau\sum_{j\in\Lambda_i^I}|\Gamma_{ij}^b|\rho_{ij}^I\mathbf{n}_{ij}^b\cdot\mathbf{q}_{ij}^b
\end{aligned}
\tag{33}
$$

Now exploiting the equations (27) we end with

$$
\begin{aligned}
&c_i\Big(|V_i|\phi_i\rho_i^{m-1} + \tau|V_i|\rho_i^+Q_i^+ + \tau\sum_{j\in\Lambda_i^I}|\Gamma_{ij}^b|\rho_{ij}^I\mathbf{n}_{ij}^b\cdot\mathbf{q}_{ij}^b\Big)\\
&\geq c_i^{m-1}|V_i|\phi_i\rho_i^{m-1} + c_i^+\tau|V_i|\rho_i^+Q_i^+ + c_i^I\tau\sum_{j\in\Lambda_i^I}|\Gamma_{ij}^b|\rho_{ij}^I\mathbf{n}_{ij}^b\cdot\mathbf{q}_{ij}^b
\end{aligned}
\tag{34}
$$

where (30) easily follows. □

Remark 4.2. For the case of different discretizations of the flow equation (1) then (27) or if (27) are not fulfilled because of some other reasons (during an iterative procedure, ...), the Theorem 4.1 needs not to be valid.

To avoid it one has to use another discretization of the transport equation that is equivalent to the origin one (23) if (27) is fulfilled and for which the discrete maximum principle can be proved without assuming (27).

We get such discretization by multiplying (27) with c_i and subtracting it from (23) when we get

$$
\begin{aligned}
&|V_i|\phi_i\rho_i^{m-1}(c_i - c_i^{m-1}) + \tau|V_i|\rho_i Q_i^+(c_i - c_i^+)\\
&\quad + \tau\sum_{j\in\Lambda_i}\sum_{e\in\Lambda_{ij}}|\Gamma_{ij}^e|\rho^e\left(\mathbf{n}_{ij}^e\cdot\mathbf{q}_{ij}^e(\gamma_{ij}^e-1/2)+\lambda_{ij}^e h_{ij}^{-1}\right)(c_i - c_j)\\
&\quad - \tau\sum_{j\in\Lambda^I}|\Gamma_{ij}^b|\rho_{ij}\mathbf{n}_{ij}^b\cdot\mathbf{q}_{ij}^b(c_i - c_i^I) = 0.
\end{aligned}
\tag{35}
$$

For the above discretization the discrete maximum principle can be proved similarly to the Theorem 4.1 without assuming (27).

The discrete equations (35) can be obtained also by considering an appropriate discretization of the equation

$$\phi\rho\partial_t c + \rho\mathbf{q}\cdot\nabla c - \nabla\cdot(\rho D\nabla c) + \rho^+ Q^+(c - c^+) = 0$$

that itself can be obtained by the similar manipulation of (3) and (1).

It is important to mention that if the discrete flow equations (27) are not fulfilled, we lose with (35) the **discrete local mass balance** that is for us represented by the discrete transport equations (23).

5. Upwind Algorithms

Full upwind appears to be appropriate only in the situations where the convection dominates strongly to the diffusion over the whole domain and time interval. For variable density flows where the velocity can vary from small values to large ones, the full upwind introduces too large modification quoted often as an **artificial diffusion**.

In such cases more sophisticated upwind methods are necessary. To explain clearly other upwind techniques we describe them for 1D case to extend them easily to R^2.

We deal next with the **total flux** made of convection and diffusion for c

$$\mathcal{J}_{ij} := q_{ij}\, c - d_{ij}\, \partial_x c,\ x \in (x_i, x_j),\ \ c(x_i) = c_i,\ c(x_j) = c_j \tag{36}$$

where q_{ij} and d_{ij} are some appropriate constants, e.g. $q_{ij} := q(x_{ij})$, $d_{ij} := d(x_{ij})$.

Substituting c in (36) by the linear interpolation $\tilde{c}$ of c_i and c_j we get the approximation

$$\mathcal{J}_{ij} \approx \tilde{\mathcal{J}}_{ij} := q_{ij}\tilde{c} - d_{ij}\partial_x\tilde{c} \tag{37}$$

with the value at the point x_{ij}

$$J_{ij} := \tilde{\mathcal{J}}_{ij}(x_{ij}) = q_{ij}\frac{c_i + c_j}{2} - d_{ij}\frac{c_j - c_i}{h_{ij}}\,. \tag{38}$$

It is well-known that the assumption of a linear profile of the numerical solution for the equations with mostly hyperbolic character is not appropriate. Following the ideas of [**12**] and [**1**] we search for another interpolation profile of c that will result in the flux that is **constant** over whole interval (x_i, x_j). It is worth to note that by using such numerical approximation we get an exact solution for the special case of equation with constant coefficients

$$\frac{\partial}{\partial x}\left(qc - d\frac{\partial c}{\partial x}\right) = 0.$$

To make generalization later easier we reformulate $\tilde{\mathcal{J}}_{ij}$ from (37) into the equivalent formulation

$$\tilde{\mathcal{J}}_{ij} \equiv q_{ij}c(s) - \frac{d_{ij}}{h_{ij}}\dot{c}(s)\,,\ s \in (0,1),\ c(0) = c_i,\, c(1) = c_j \tag{39}$$

where

$$c(s) := c(x(s)),\ \dot{c}(s) := \frac{\partial c(s)}{\partial s},\ x(s) := x_i + sh_{ij},\ h_{ij} := x_j - x_i\ .$$

Introducing the **local Peclet number**

$$P_{ij} := \frac{h_{ij}q_{ij}}{d_{ij}}$$

we see that if we substitute $c(s)$ in (39) by the **exponential** function

$$c^*(s) = c_i + (c_j - c_i)\frac{\exp(P_{ij}s) - 1}{\exp(P_{ij}) - 1} \tag{40}$$

the total flux $\mathcal{J}^*_{ij} := q_{ij}c^*(s) - d_{ij}\dot{c}^*(s)$ takes (if $P_{ij} \neq 0$) for any $s \in (0,1)$ the **constant** value J^*_{ij}

$$J^*_{ij} := c_i q_{ij}\left(1 + \frac{1}{\exp(P_{ij}) - 1}\right) - c_j q_{ij}\left(\frac{1}{\exp(P_{ij}) - 1}\right). \tag{41}$$

Approximating the convective-diffusive flux between the nodes x_i and x_j by (41) also in the case of general 1D equation leads to so called **exponential upwind scheme** [**12**].

After simple algebraic manipulations we obtain an equivalent form to (41) (if $d_{ij} \neq 0$)

$$J^*_{ij} \equiv q_{ij}\frac{c_i + c_j}{2} - \mathcal{K}_{ij}d_{ij}\frac{c_j - c_i}{h_{ij}} \tag{42}$$

where

$$\mathcal{K}_{ij} := \frac{P_{ij}}{2} + \frac{P_{ij}}{\exp(P_{ij}) - 1} \tag{43}$$

with the natural extension $\mathcal{K}_{ij} = 1$ for $P_{ij} = 0$.

The approximation (42) can be considered as an addition of the artificial diffusion $(\mathcal{K}_{ij} - 1)d_{ij} \geq 0$ to the diffusion d_{ij} in the approximation of the flux by the "standard" form (38).

There exist several other upwind methods that do not use the "exact" exponential interpolation profile (40), but some appropriate approximation of it, see [**12**] for a **power-law scheme**, [**7**] for a **partial upwind scheme** or [**1**] for a general scheme with many other examples.

Also the full upwind scheme from the previous chapter can be formulated in the form (42) with

$$\mathcal{K}_{ij} := 1 + \frac{|P_{ij}|}{2} \ . \tag{44}$$

Finally, the partial upwind scheme [**7**] (or equivalent **hybrid upwind scheme** [**12**]) is defined by

$$\mathcal{K}_{ij} := \max\left\{1, \frac{|P_{ij}|}{2}\right\} . \tag{45}$$

All forms of (42) with different $\mathcal{K}_{ij}$ can be introduced only by assuming strictly $d_{ij} \neq 0$. For purely convective case one has to apply the full upwind scheme as it is described in the previous section.

The partial upwind scheme is "optimal" from a heuristic point of view that it modifies the origin discretization (38) by an "addition" of minimal amount of the artificial diffusion to ensure the discrete maximum principle. In fact it contains the criterion that if all local Peclet numbers in absolute value are smaller then 2, no modifications are necessary.

On other hand the full upwind scheme introduces always too large modification, especially for medium values of local Peclet numbers, see the Figure 2. for a comparision of $\mathcal{K} = \mathcal{K}(P)$ for different upwind methods.

The upwind schemes can be viewed also in a formulation analogous to (21) where the diffusive part is unmodified and the concentration at the convective part is substituted by some value between c_i and c_j. The equivalent form to (42) with all choices (43)–(45) of K_{ij} available is then defined by

$$J^*_{ij} \equiv q_{ij}\left(c_i\left(\frac{1}{2} + \frac{\mathcal{K}_{ij} - 1}{P_{ij}}\right) + c_j\left(\frac{1}{2} - \frac{\mathcal{K}_{ij} - 1}{P_{ij}}\right)\right) - d_{ij}\frac{c_j - c_i}{h_{ij}} \tag{46}$$

where we must assume $P_{ij} \neq 0$, i.e. $q_{ij} \neq 0$.

For R^2 all above ideas can be straightforwardly implemented only for a special situation. We search for a substitution of the flux $\tilde{\mathcal{J}}^e_{ij}$ considered at the line $x = x_i + s(x_j - x_i),\ s \in (0,1)$ and defined by

$$\tilde{\mathcal{J}}^e_{ij} := \mathbf{n}^e_{ij} \cdot \left(\mathbf{q}^e_{ij}\tilde{c}(x(s)) - D^e \cdot \nabla\tilde{c}(x(s))\right) \tag{47}$$

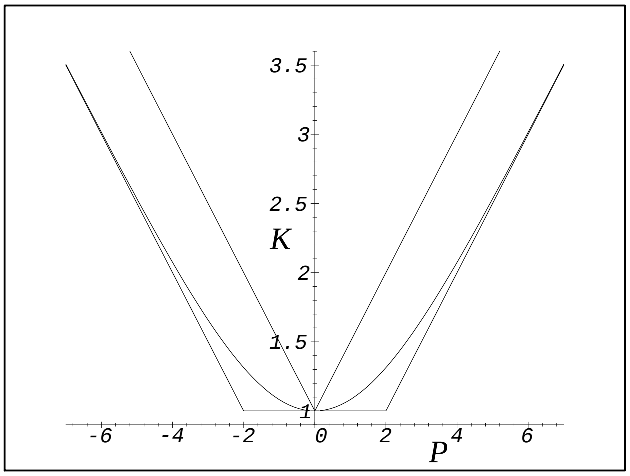

Figure 2. The full (the upper curve), exponential and partial upwind.

with the value $\tilde{J}^e_{ij}$ at x_{ij}

$$\tilde{J}^e_{ij} := \tilde{\mathcal{J}}^e_{ij}(x_{ij}) = \mathbf{n}^e_{ij} \cdot \left(\mathbf{q}^e_{ij} \frac{c_i + c_j}{2} - D^e \cdot \nabla \tilde{c}|_{T^e} \right) . \tag{48}$$

For the case of Voronoi diagrams and an isotropic diffusion $D^e = d^e I$ we can utilize that the direction of $\mathbf{n}^e_{ij}$ coincides with the direction of the edge connecting x_i and x_j and we have an analytical relation

$$\mathbf{n}^e_{ij} \cdot \nabla c(x(s)) = \frac{1}{h_{ij}} \partial_s c(x(s)).$$

We can now write analogously to (39) that (47) is equivalent to

$$\tilde{\mathcal{J}}^e_{ij} \equiv \mathbf{n}^e_{ij} \cdot \mathbf{q}^e_{ij}\, c(s) - \frac{d^e}{h_{ij}}\, \dot{c}(s)\,,\ \ s \in (0,1),\ \ c(0) = c_i,\ c(1) = c_j. \tag{49}$$

Now all ideas from 1D case can be applied. Denoting the local Peclet number to be

$$P^e_{ij} := \frac{h_{ij} \mathbf{n}^e_{ij} \cdot \mathbf{q}^e_{ij}}{d^e} \tag{50}$$

one can substitute the flux (48) by

$$\tilde{J}^{*e}_{ij} := \mathbf{n}^e_{ij} \cdot \mathbf{q}^e_{ij} \frac{c_i + c_j}{2} - \mathcal{K}^e_{ij} d^e \frac{c_j - c_i}{h_{ij}} \tag{51}$$

where all analogous definitions (43), (44) and (45) of $\mathcal{K}^e_{ij}$ can be used.

Similar to (46) we can reformulate (51) to the equivalent formulation

$$\tilde{J}^{*e}_{ij} \equiv \mathbf{n}^e_{ij}\mathbf{q}^e_{ij}\left(c_i\left(\frac{1}{2}+\frac{\mathcal{K}^e_{ij}-1}{P^e_{ij}}\right)+c_j\left(\frac{1}{2}-\frac{\mathcal{K}^e_{ij}-1}{P^e_{ij}}\right)\right)-d^e\frac{c_j-c_i}{h_{ij}}\,. \tag{52}$$

For general finite volumes the flux (47) can not be expressed in the form (49). Nevertheless the approximation (52) can be used instead of (24), see [**1**] for details, but the discrete maximum principle is then fulfilled only for full upwind scheme.

Here we present a new formulation of (24) where we exploit the relation (17) and where all upwind schemes for arbitrary node-centered FVM construction can be applied with the valid discrete maximum principle.

Using the definition of λ^e_{ij} by (16) we introduce a proper definition of the "flux"

$$\mathcal{J}^e_{ij} := \mathbf{n}^e_{ij}\cdot\mathbf{q}^e_{ij}c(s)-\frac{\lambda^e_{ij}}{h_{ij}}\,\dot{c}(s) \tag{53}$$

where $c(s)=c_i+s(c_j-c_i)$, $s\in(0,1)$. From (17) we have that the new definition (53) is related to the "standard" (48) through

$$\sum_{j\in\Lambda^e_i}|\Gamma^e_{ij}|\tilde{J}^e_{ij}=\sum_{j\in\Lambda^e_i}|\Gamma^e_{ij}|\mathcal{J}^e_{ij}(1/2)\,. \tag{54}$$

With (53) in mind all upwind techniques can be applied. Defining

$$P^e_{ij} := \frac{h_{ij}\mathbf{n}^e_{ij}\cdot\mathbf{q}^e_{ij}}{\lambda^e_{ij}}$$

we get the approximation

$$J^{*e}_{ij} := \mathbf{n}^e_{ij}\cdot\mathbf{q}^e_{ij}\frac{c_i+c_j}{2}-\mathcal{K}^e_{ij}\lambda^e_{ij}\frac{c_j-c_i}{h_{ij}} \tag{55}$$

or the equivalent one

$$J^{*e}_{ij} \equiv \mathbf{n}^e_{ij}\mathbf{q}^e_{ij}\left(c_i\left(\frac{1}{2}+\frac{\mathcal{K}^e_{ij}-1}{P^e_{ij}}\right)+c_j\left(\frac{1}{2}-\frac{\mathcal{K}^e_{ij}-1}{P^e_{ij}}\right)\right)-\lambda^e_{ij}\frac{c_j-c_i}{h_{ij}} \tag{56}$$

where all analogous definitions (43), (44) and (45) of $\mathcal{K}^e_{ij}$ can be applied.

Substituting (24) by (56) the discrete maximum principle can be now proved similarly to the Theorem 4.1 in the previous section.

Using (54) one can **formally** express the contribution of two fluxes J^{*e}_{ij} and J^{*e}_{il} for $j,l\in\Lambda^{e,i}$ as an addition of the **local** artificial diffusion ϵ^e_{ij} in $\tilde{J}^e_{ij}$ and ϵ^e_{il} in $\tilde{J}^e_{il}$

to the diffusion D^e in the standard approximation (48). To do so one should solve the linear system

$$\epsilon_{ij}^e|\Gamma_{ij}^e|\mathbf{n}_{ij}^e \cdot \nabla N_j^e + \epsilon_{il}^e|\Gamma_{il}^e|\mathbf{n}_{il}^e \cdot \nabla N_j^e = \frac{\lambda_{ij}^e}{h_{ij}}(\mathcal{K}_{ij}^e - 1); \tag{57}$$

$$\epsilon_{ij}^e|\Gamma_{ij}^e|\mathbf{n}_{ij}^e \cdot \nabla N_l^e + \epsilon_{il}^e|\Gamma_{il}^e|\mathbf{n}_{il}^e \cdot \nabla N_l^e = \frac{\lambda_{il}^e}{h_{il}}(\mathcal{K}_{il}^e - 1). \tag{58}$$

It is important to remark that if the angle in T^e opposite to the edge connecting x_i and x_j is $\pi/2$ then $\lambda_{ij}^e = 0$. In such situation the full upwind scheme from the previous section must be applied although D^e in general needs not to be zero.

For the grids made strictly of equilateral triangles when Donald and Voronoi diagrams coincide and for $D = dI$ we have $\lambda_{ij}^e \equiv d^e$.

6. Numerical Experiments

All previous results appear useful in numerical simulations of density driven flows. In fact the study of the subjects was motivated by real numerical difficulties when applying "standard" computational methods.

The following numerical simulations were computed using the software package **UG** [**3**] with an implementation of finite volume discretization (23) and (27) using Donald diagrams and consistent velocity approximation [**5**].

First numerical test that we present here to illustrate different upwind algorithms is so called "Elder example". Although its origin comes from thermodynamical simulations, because of his complex behaviour it has become a standard benchmark also for software packages simulating a mass transfer with variable density flows.

The computational domain of the example in a nondimensional form is a quadrangle of size 4×1 where at the top boundary ($y = 1$) the concentration is fixed at the middle part ($c(x, 1) = 1,\ x \in [2, 3]$) and at all other parts of boundary the concentration is set to $c = 0$. The domain is supposed to be isolated at the boundary ($\mathbf{n} \cdot \mathbf{q} = 0$) except at the top left and right corners where a mass inflow is allowed by fixing the pressure. The initial concentration is $c(x, 0) \equiv 0$. For other data and details see [**11**].

Because of the variation of c near the top boundary the velocities develop due to the variation of ρ in (2) and they close themselves in recirculation cells. Further due to the convection-diffusion transport of brine into the domain, so called "fingers" of brine appear that are accompanied each by two recirculation cells, see the Figure 3, where numerical results due to the symmetry are presented only for the left half of the domain.

The dynamical behaviour of Elder example is very complex with the velocity $\mathbf{q}$ exhibiting a large variation in time and space.

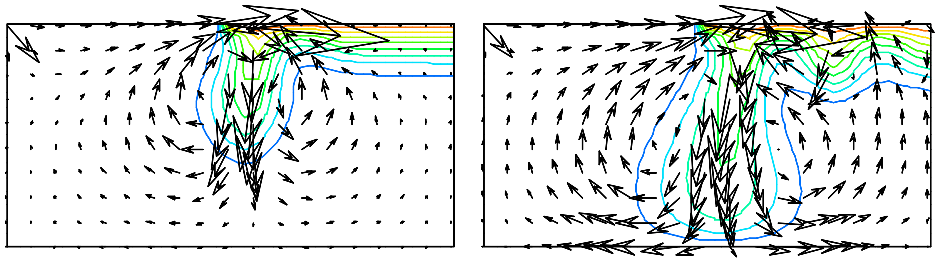

Figure 3. Numerical solutions at different times for Elder example.

We compared different upwind algorithms for the Elder example. The grid was created by an "advancing front" algorithm with most of triangles almost equilateral. First, numerical simulations with no upwind were computed. The grid seemed to be fine "enough" as some (negative) oscillations appeared only inside of small areas near the boundary with the fixed large gradient of concentration (see the Figure 4), but where they reached large magnitudes (about 30%).

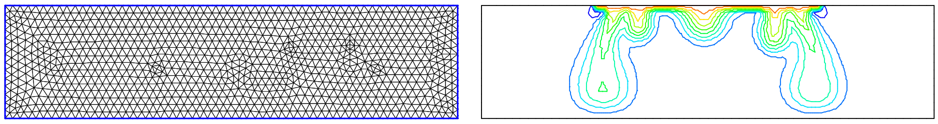

Figure 4. Grid and numerical solution for no upwind.

Stabilizing the Elder example by full upwind resulted in qualitatively very different numerical results. As full upwind added an unnecessary large amount of "artificial" diffusion, the numerical solution was during time simulation too diffusive that resulted into a different number of the fingers for this grid. On the other hand, the simple algorithm of partial upwind scheme gave analogous numerical results with respect to no upwind method, but with no oscillations presented (see the Figure 5).

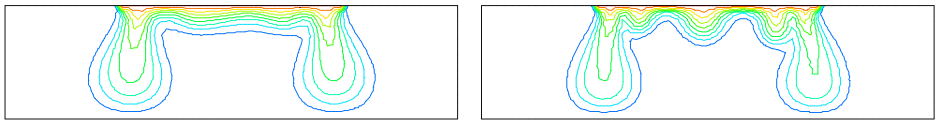

Figure 5. Comparison of the full and partial upwind.

To illustrate next the necessity of careful treatments of coupled boundary conditions we present another example, so called "Saltdome" benchmark [**11**].

Here the domain is the quadrangle of size 3×1. The (nondimensional) pressure is given at the top boundary by setting a linear relation $p(x, 1) = 2 - x/3$, otherwise isolated boundaries are supposed ($\mathbf{n}\cdot\mathbf{q}=0$). The concentration is fixed at the bottom part ($c(x,0)=1$, $x\in[1,2]$) and at the rest part of the bottom boundary and on the sides "no flux" condition is supposed. On the top boundary the "inflow/outflow" boundary conditions (8) and (7) are prescribed where for an inflow regime the concentration is fixed $c=0$. The initial situation is again $c(x,0)\equiv 0$.

As the values of pressure at the vertices lying on the top boundary are given by Dirichlet boundary conditions, using a "standard" approach the discrete flow equations (27) are not computed there. The fluxes $\mathbf{n}^b_{ij}\cdot\mathbf{q}^b_{ij}$ at Γ^O, used in outflow boundary conditions for c, are computed simply from a discrete form of Darcy's law (2) and not from (27), so consequently the discrete mass balance equations (27) are not fulfilled there.

For such case no discrete maximum principle needs to be valid with arbitrary upwind algorithm for any grid and an unrealistic behaviour for the concentration at the right top corner, see the Figure 6, is then no surprise. There one can observe a nonphysical "inflow" of the concentration from outside even before it "arrives" there from bottom. An answer to the most important question of the Saltdome example about a time at which some significant value of the brine concentration arrives at the top boundary, has then minimal reliability.

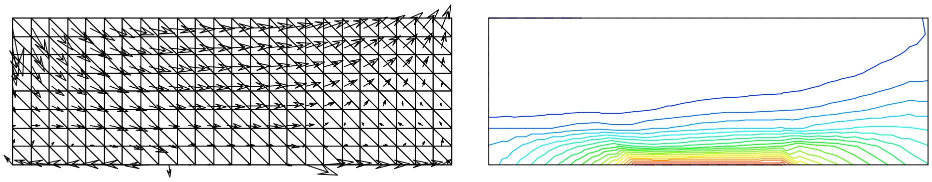

Figure 6. Velocity field and concentration contours for Saltdome example.

In fact if one continue with numerical simulations, the amount of artificial concentration at the top right corner during time evolution is so large that it results in an instable situation when the computations corrupt.

Considering the flux $\mathbf{n}^b_{ij}\cdot\mathbf{q}^b_{ij}$ in outflow boundary conditions for c that fulfil (27) or using the discretization (35) excludes this numerical artifact.

References

1. Angermann L., *An introduction to finite volume methods for linear elliptic equations of second order.*, Preprint 164, Institut für Angewandte Mathematik, Universität Erlangen, Februar 1995.
2. ———, *An upwind scheme of finite volume type with reduced crosswind diffusion.*, Preprint 165, Institut für Angewandte Mathematik, Universität Erlangen, Juli 1995.
3. Bastian P., Birken K., Eckstein K., Johannsen K., Lang S., Neuss N. and Rentz-Reichert H., *Ug — a flexible software toolbox for solving partial differential equations*, Computing and Visualization in Science **1**(1) (1997), 27–40.
4. Bear J., *Dynamics of Fluids in Porous Media*, Dover Publication, Inc., New York, 1988.

5. Frolkovič P., *Finite volume discretizations of density driven flows in porous media*, Finite Volumes for Complex Applications (Vilsmeier R. Benkhaldoun F., eds.), Hermes, Paris, 1996, pp. 433–440.
6. Hackbusch W., *On first and second order box schemes.*, Computing **41** (1989), 277–296.
7. Ikeda T., *Maximum principle in finite element models for convection-diffusion phenomena*, North-Holland, Amsterdam, New York, Oxford, 1983.
8. Johannsen K., *Aligned 3d-finite-volumes for convection-diffusion-problems*, Finite Volumes for Complex Applications (Vilsmeier R. Benkhaldoun F., eds.), Hermes, Paris, 1996, pp. 291–300.
9. Knabner P. and Frolkovič P., *Consistent velocity approximations in finite element and volume discretizations of density driven flow in porous media.*, Computational Methods in Water Resources XI (Aldama A. A. et al.,, eds.), Computational Mechanics Publications, Southampton, Boston, 1996, pp. 93–100.
10. Leijnse A., *Three-dimensional modeling of coupled flow and transport in porous media*, PhD thesis, University of Notre Dame, Indiana, 1992.
11. Oldenburg C. M. and Pruess K., *Dispersive transport dynamics in a strongly coupled groundwater-brine flow system*, Water Resour. Res. **31**(4) (1995), 289–302.
12. Patankar S. V., *Numerical heat transfer and fluid flow*, Hemisphere Publishing Corporation, 1980.
13. Wei Y., *Stabilized finite element methods for miscible displacement in porous media*, R.A.R.I.O. Modél. Math. Anal. Numér **28**(5) (1994), 611–665.

P. Frolkovič, Department of Applied Mathematics, Friedrich-Alexander-Universität Erlangen-Nürnberg, Martensstrasse 3, 91058 Erlangen, Germany; *e-mail:* frolkovi@am.uni-erlangen.de; `http://www.am.uni-erlangen.de/~frolkovi`